Humanization of the Blood–Brain Barrier Transporter ABCB1 in Mice Disrupts Genomic Locus — Lessons from Three Unsuccessful Approaches

Markus Krohn[1*], Thomas Wanek[2], Marie-Claude Menet[3], Andreas Noack[4], Xavier Declèves[3], Oliver Langer[2,5,6†], Wolfgang Löscher[4,7†] and Jens Pahnke[1,8,9,10†]

[1]*Translational Neurodegeneration Research and Neuropathology Lab, Department of Neuro-/Pathology, University of Oslo and Oslo University Hospital, Oslo, Norway*
[2]*Center for Health and Bioresources, AIT Austrian Institute of Technology GmbH, Seibersdorf, Austria*
[3]*Inserm UMR-S 1144, Faculté de Pharmacie, Université Paris Descartes, Paris, France*
[4]*Department of Pharmacology, Toxicology, and Pharmacy, University of Veterinary Medicine, Hannover, Germany*
[5]*Department of Clinical Pharmacology, Medical University of Vienna, Vienna, Austria*
[6]*Department of Biomedical Imaging and Image-guided Therapy, Division of Nuclear Medicine, Medical University of Vienna, Vienna, Austria*
[7]*Center for Systems Neuroscience, Hannover, Germany*
[8]*LIED, University of Lübeck, Lübeck, Germany*
[9]*Department of Bioorganic Chemistry, Leibniz-Institute of Plant Biochemistry, Halle, Germany*
[10]*Department of Pharmacology, University of Latvia, Riga, Latvia*

Received: 17 April 2018; accepted: 16 May 2018

ATP-binding cassette (ABC) transporters are of major importance for the restricted access of toxins and drugs to the human body. At the body's barrier tissues like the blood–brain barrier, these transporters are highly represented. Especially, ABCB1 (P-glycoprotein) has been a priority target of pharmaceutical research, for instance, to aid chemotherapy of cancers, therapy resistant epilepsy, and lately even neurodegenerative diseases. To improve translational research, the humanization of mouse genes has become a popular tool although, like recently seen for *Abcb1*, not all approaches were successful. Here, we report the characterization of another unsuccessful commercially available *ABCB1* humanized mouse strain. In vivo assessment of transporter activity using positron emission tomography imaging revealed a severe reduction of ABCB1 function in the brain of these mice. Analyses of brain mRNA and protein expression showed that the murine *Abcb1a* gene is still expressed in homozygous humanized animals while expression of the human gene is minimal. Promoter region analyses underpinned that the introduced human gene might dysregulate normal expression and provided insights into the regulation of both transcription and translation of *Abcb1a.* We conclude that insertion of the human coding DNA sequence (CDS) into exon 3 instead of exon 2 most probably represents a more promising strategy for *Abcb1a* humanization.

Keywords: ABCB1, P-gp, ABC transporter, PET imaging, mouse models, humanization

Introduction

Although most of the ATP-binding cassette (ABC) transporter family members are not linked to multidrug resistance, the probably most prominent one, ABCB1 (P-gp), is mainly known for its role in therapy resistant cancer. However, during the past 30 years, it became evident that it is not only of major importance for controlling access of cancer therapies to tumors, but that ABCB1 (1) has a pronounced impact on drug distribution, excretion, and drug–drug interactions [1–3]; (2) is a stem cell marker [4–6]; (3) is linked to therapy resistant epilepsy and depression [7]; (4) is involved in the pathogenesis of neurodegenerative diseases [8–11]; and (5) is essential in a number of signaling pathways [5, 12–14]. In mice, the *Abcb1* gene underwent a duplication resulting in the two isoforms *Abcb1a* and *Abcb1b*. The proteins share 87.3% and 80.5% identical amino acids, respectively, to human ABCB1, and several substrate specific differences were identified regarding affinity and specificity [15–17]. Although in vitro assays exist to assess the interaction of drugs with ABCB1 and predict certain in vivo characteristics of a substance, most drug development pipelines include mouse in vivo studies to assess pharmacokinetics, metabolism, toxicity, and side effects of new drugs [18]. To eliminate uncertainties of inter-species differences, humanized mouse models are being deployed recently [19]. Dallas et al. [20] reported the successful humanization of the *Abcg2* gene in mice by exchanging the 107 kbp mouse gene for the 141 kbp human gene. The approach may suffer from the unpredictability of disrupting long-range transcriptional elements or possible incompatibilities between mouse and human binding sites. This, most probably, is the reason for the reported reduced protein expression in major organs. However, the model seems clearly useful for drug development and drug–drug interaction studies [20]. Sadiq et al. [21] published data on a humanized *ABCB1* mouse model from Taconic using a fusion of the human *ABCB1* coding DNA sequence (CDS) directly behind the start codon of both the *Abcb1a* and *Abcb1b* genes, instead of full humanization of the respective gene loci. Exhaustive protein expression analyses revealed that the human protein was

* Corresponding author: Department for Neuro/Patologi, Oslo Universitetssykehus HF, Rikshospitalet, A2.M051, Postboks 4950 Nydalen, 0424 Oslo, Norway; E-mail: markuskrohn@gmail.com; Tel: +4723071478; Fax: +4723071410.
† These authors shared last authorship.

DOI: 10.1556/1886.2018.00008

expressed at negligible levels at the blood–brain barrier (BBB) while other proteins were not influenced. Interestingly, the murine ABCB1A protein was detected at only 10% of the wild-type level, but still about 7-fold higher than the human protein. Accordingly, the humanized *ABCB1* mice rather resembled *Abcb1a/b* knockout mice than wild-type animals when assessing the brain distribution of several ABCB1 substrates [21]. Due to the increasing importance of ABCB1 in Alzheimer's disease (AD) and the increasing number of failed AD treatment trials, we set out to find another ABCB1 humanized mouse model that could serve as a basis for new AD mouse models. Here, we report the characterization of a second commercially available *ABCB1* humanized mouse model that has been developed by genOway (Lyon, France) almost in parallel to the one reported by Sadiq et al. [21].

Materials and Methods

Mouse Models. Humanized ABCB1 mice in C57BL/6 background (hABCB1) have been purchased from genOway S.A. (Lyon, France) and from TaconicArtemis GmbH (Cologne, Germany) [21]. C57BL/6J wild-type and B6.C-Tg(CMV-cre)1Cgn/J (Cre-deleter) mice have been purchased from The Jackson Laboratory (Bar Harbor, USA). DNA sequencing data acquired during this study revealed that the human ABCB1 coding sequence in hABCB1 mice had been flanked by loxP sites. To induce hABCB1 knockout, we crossbred hABCB1 to Cre-deleter mice. The resulting homozygous knockout mice are referred to as human *ABCB1*$^{-/-}$ mice. All strains have been bred and housed under SOPF (specific and opportunistic pathogen-free) conditions at 21 ± 1 °C, 12 h/12 h light/dark cycle with food (PM3, Special Diet Services) and acidified water ad libitum. Genotyping of mice was done on ear biopsies employing a three-primer PCR that differentiated wild-type, knock-in, and knock-out mice (primers: humB1fw: 5′-GGCGTAGATTGAGCATGCTA-3′, humB1rc: 5′-AAAACACCGTCCTGAAAGCT-3′, humB1ko: 5′-AACAGCATATGGCTCAGGTG-3′). All protocols involving the breeding and use of animals were approved by the Landesverwaltungsamt Sachsen-Anhalt, Halle, Germany; the Norwegian Food Safety Authority (Mattilsynet); and the Austrian authority (Amt der Niederösterreichischen Landesregierung). All study procedures were performed in accordance with the European Communities Council Directive of September 22, 2010 (2010/63/EU).

Positron Emission Tomography (PET) Imaging

General. Tariquidar dimesylate was obtained from Xenova Ltd. (Slough, UK). For PET experiments, tariquidar was freshly dissolved prior to each administration in 2.5% (w/v) aqueous (aq.) dextrose solution and injected i.v. at a volume of 4 mL/kg body weight. (*R*)-[^{11}C]verapamil was synthesized as described before [22] and formulated for i.v. injection in physiological saline solution (0.9%, w/v) containing 1% (v/v) Tween 80 at an approximate concentration of 370 MBq/mL. Specific activity at end of synthesis was 137 ± 34 GBq/μmol, and radiochemical purity was >98%.

Imaging Procedures. Groups of female C57BL/6N mice (age, 14–16 weeks), hABCB1 mice (genOway), and hABCB1 mice (TaconicArtemis GmbH) were either i.v. injected with vehicle solution (2.5% [w/v] aq. dextrose solution) or 15 mg/kg body weight tariquidar at 2 h before start of PET imaging (n = 3–6 per group). For injection, mice were pre-anesthetized in an induction chamber using isoflurane (2.5–3.5% in oxygen) and placed on a heated animal bed (38 °C), and the lateral tail vein was cannulated. Animal respiratory rate and body temperature were constantly monitored (SA Instruments Inc., Stony Brook, NY, USA), and the isoflurane level was adjusted (1.5–2% in oxygen) to achieve a constant and sufficient depth of anesthesia. Anesthesia was maintained for the whole pre-treatment and imaging period. Following administration, the animal bed was transferred into the gantry of a microPET scanner (Focus 220, Siemens Medical Solutions, Knoxville, TN, USA) and a 10-min transmission scan using a ^{57}Co point source was recorded. Subsequently, at 2 h after tariquidar or vehicle injection, (*R*)-[^{11}C] verapamil (32 ± 9 MBq, <0.5 nmol, 0.1 mL) was administered as an i.v. bolus over 1 min, and a 60 min dynamic PET scan (energy window, 250–750 keV; timing window, 6 ns) was initiated at the start of radiotracer injection. After completion of the imaging procedure, a terminal blood sample was withdrawn under isoflurane anesthesia from the retro-orbital sinus vein and the animals were sacrificed by cervical dislocation. Blood was measured for radioactivity in a gamma counter (Wizard 1470, Perkin-Elmer, Wellesley, MA, USA).

PET Data Analysis. The 60 min dynamic emission PET data were sorted into 23 frames, which incrementally increased in time length from 5 s to 10 min. Images were reconstructed using Fourier rebinning of the 3D sonograms followed by two-dimensional filtered back projection with a ramp filter, resulting in an image voxel size of 0.4 × 0.4 × 0.796 mm. A standard data correction protocol (normalization, attenuation and decay correction) was applied to the PET data. The PET units were converted into units of radioactivity concentration by applying a calibration factor derived from imaging of a cylindrical phantom with a known ^{11}C-radioactivity concentration. Using the image analysis software Amide [23], whole brain was manually outlined on the PET images, and time-activity curves, expressed in standardized uptake value ((radioactivity per g/injected radioactivity) × body weight), were derived. Individual brain-to-blood concentration ratios ($K_{b,brain}$) were calculated by dividing the brain radioactivity concentration in the last PET frame (50 to 60 min after radiotracer injection) by the corresponding blood radioactivity concentration as determined by the gamma counter measurements.

Quantitative PCR. Mice were sacrificed by cervical dislocation. After quick intracardial perfusion with 10 mL ice-cold PBS, one hemisphere of each brain was snap-frozen in liquid nitrogen within 3 min after death. Brains of 100-day- and 200-day-old wild-type male mice (3 and 4, respectively) and hABCB1 male mice (5 each) were preserved using Allprotect® Tissue Reagent (Qiagen, Germany). Total RNA was isolated using the RNeasy® Mini Kit (Qiagen, Germany). RNA concentrations were assessed photometrically. cDNA was synthesized using the High Capacity RNA-to-cDNA Kit (Applied Biosystems, USA). Gene expression was analyzed with qRT-PCR using TaqMan Hybridization Probes. Primer sets with according TaqMan probes for *Abcb1a* (Mm00440761_m1), human *ABCB1* (Hs00184500_m1), and mouse *Actb* (Mm02619580_g1) genes were purchased from Thermo Fisher Scientific Inc. (USA). Gene expression was normalized to the housekeeping gene actin. All 17 cDNA samples were tested with each primer (*Abcb1a*, human *ABCB1*, and *Actb*), including a non-template control. Reactions were composed according to manufacturer's instructions with a final volume of 20 μL and 30 ng of template. PCR amplification conditions were 50 °C for 2 min, 95 °C for 10 min, 40 cycles of 95 °C for 15 s, and 60 °C for 1 min. For comparison of expression values between strains, the unpaired Student's t test has been used. For analyses of transcript variants, RNA of a new set of brains was prepared from female wild-type, hABCB1, and human *ABCB1*$^{-/-}$ mice (5 each) and assayed using the mentioned assay and conditions plus assays Mm00440745_m1 and Mm00440751_m1.

Protein Quantification (QTAP)

Reagents. HBSS, HEPES, Tris-HCl, and sodium phosphate (Na_2HPO_4 and NaH_2PO_4) were provided by Sigma-Aldrich

(Saint Quentin Fallavier, France). The reagents used for plasma membrane isolation and protein digestion, NaCl, $MgCl_2$, KCl, sucrose, EDTA, guanidine–HCl, DTT, iodoacetamide, and urea also came from Sigma-Aldrich (Saint Quentin Fallavier, France). The complete Mini (EDTA-free) Protease Inhibitor Cocktail tablets were provided by Roche (Bâle, Switzerland). Chloroform (HiPerSolv, Chromanorm for high-performance liquid chromatography [HPLC]) was supplied by VWR (Strasbourg, France). HPLC-grade acetonitrile and methanol were purchased at Merck (Nogent-sur-Marne, France). Formic acid (99% w/w), HPLC grade, was supplied by Fischer Scientific (Illkirch, France). All the water was prepared with a Milli-Q water purification system (Millipore, Molsheim, France). Sequencing grade modified trypsin, mass spectrometry grade rLys-C, and ProteaseMAX surfactant were from Promega (Charbonnières-les-Bains, France). The measurement of protein concentration was carried out by using the Micro BCA Protein Assay Kit (Thermo Scientific, Illkirch, France). The standard solutions of peptides were provided by UMR 8638, Chimie Organique Médicinale et Extractive — Toxicologie Expérimentale or by Pepscan (Lelystad, The Netherlands).

Plasma Membrane Protein (PMP) Fractionation. PMP fractions of mouse brains were obtained as previously described with minor modifications [20, 24]. The frozen brains were thawed at 4 °C, and all the following steps were performed on ice. The samples were washed at least twice by using an isotonic buffer solution (10 mM phosphate buffer pH 7.4, 0.1 M KCl) supplemented with Protein Inhibitor Cocktail, minced with scalpels until obtaining 1 mm pieces and homogenized with an Ultraturrax® (IKA®-Werke GmbH & Co. KG, Staufen, Germany) for 2 min. The homogenates were centrifuged (15 min at 10,000*g*); the supernatants were transferred to ultracentrifuge tubes and centrifuged (60 min at 100,000*g*). The pellet, corresponding to the total membrane fraction, was suspended in 250 mM sucrose buffer (with 20 mM Tris pH 7.4 and 5.4 mM EDTA) and deposited on top of a 38% (w/v) sucrose solution. After ultracentrifugation (30 min at 100,000), the turbid layer at the interface was collected, suspended in 250 mM sucrose buffer and ultracentrifuged (30 min at 100,000). The pellet corresponding to the plasma membrane fraction was recovered in 250 mM sucrose buffer containing protease inhibitor cocktail.

Protein Digestion. The plasma membrane fractions were digested as described previously without modifications [25–27]. Briefly, 50 μg of proteins was solubilized in denaturing buffer (7 M guanidine hydrochloride, 10 mM EDTA, 500 mM Tris pH 8.5), reduced by DTT and alkylated by iodoacetamide. The alkylated proteins were precipitated with methanol–chloroform–water and resolubilized in 1.2 M urea and 0.1 M Tris, pH 8.5. Samples were first digested by using rLysC endoprotease (enzyme:protein ratio = 1:50) for 3 h at room temperature. Then trypsin (enzyme–protein ratio = 1:100) and 0.05% (w/v) ProteaseMAX were added, and samples were incubated at 37 °C overnight. The reaction was stopped by adding formic acid (3 μL at 99%, v/v). The stable isotope-labeled peptide mixture (750 fmol of each labeled peptide) was added in tryptic digest before ultrahigh-performance liquid chromatography–tandem mass spectrometry (UHPLC–MS/MS) analysis.

Protein Quantification by UHPLC–MS/MS. The proteins were quantified by the determination of the peptide concentration by using UHPLC–MS/MS with multiplexed selected reaction monitoring (SRM) method. Each peptide analyzed was specific to each protein and released after protein digestion by trypsin. The selected peptides for Abcb1a (LANDAAQVK), Abcb1a/b (IATEAIENFR), ABCB1 (FYDPLAGK), and GFAP (LDQLTANSAR); common peptide for Na^+/K^+ATPase α1/α2/α3 (AAVPDAVGK); and specific peptides for Na^+/K^+ATPase a1 (IVEIPFNSTNK), Na^+/K^+ATPase a2 (GIVIATGDR), and Na^+/K^+ATPase a3 (GVVVATGDR) were already reported by Hoshi et al. [25], Kamiie et al. [28], and Chaves et al. [29]. The samples were injected into an Acquity UPLC® system (Waters, Manchester, UK), equipped with an Acquity UPLC BEH® C18 column (Peptide BEH® C18 Column, 300Å, 1.7 μm, 2.1 mm × 100 mm) supplied by Waters (Guyancourt, France). The mobile phase consisted of a mixture of water (formic acid 0.1%, v/v) and ACN. It was operated with a flow rate of 0.5 mL/min in gradient mode, at a temperature of 30 °C. The total duration of analysis was 30 min.

Data were recorded with a Waters Xevo® TQ-S mass spectrometer (Waters, Manchester, UK). Measurements were performed by using positive electrospray ionization (ESI) with ion spray capillary voltage at 2.80 kV. Drying gas temperature was set to 650 °C at a flow rate of 800 L/h. Detection was performed in multiplexed SRM mode by using three transitions per native or labeled peptide. Skyline software [30, 31] was used for the optimization of the specific transition parameters (i.e., collision energy [CE] and peak integration). The area ratios light to labeled peptide were exported from Skyline, and the quantification was performed from calibration curves. Each sample contained two hemi cortices from different mice. It was digested in triplicate, and each triplicate was injected once. Therefore, the calculated concentrations (Table 1) take into account the experimental and biological variability.

Western Blot. Mice were sacrificed by cervical dislocation. After quick intracardial perfusion with 10 mL ice-cold PBS, one hemisphere of each brain was snap-frozen in liquid nitrogen within 3 min after death. Hemispheres of three 100-day-old male mice of each genotype were preserved using Allprotect® Tissue Reagent (Qiagen, Germany). After removal of Allprotect® reagent, brains were homogenized using a bead homogenizer

Table 1. Protein quantitation

Protein	Mouse ABCB1A/B	Mouse ABCB1A	Human ABCB1	Mouse ATP1A1	Mouse ATP1A2	Mouse ATP1A3	Mouse GFAP
Peptide	IATEAIENFR	LANDAAQVK	FYDPLAGK	IVEIPFNSTNK	GIVIATGDR	GVVVATGDR	LDQLTANSAR
Strain	Concentration [fmol/μg total protein] (CV [%])						
LoD/LoQ	0.05/0.16	0.08/0.23	0.23/0.70	0.58/1.73	0.04/0.12	0.07/0.25	0.19/0.28
hABCB1	<LoD	<LoD	<LoQ	131.5 (34.9)	86.0 (19.2)	435.2 (26.9)	1.0 (14.0)
hABCB1$^{-/-}$	0.44 (30.6)	0.36 (14.4)	<LoD	106.8 (17.0)	78.8 (13.8)	371.6 (11.0)	1.0 (32.0)
WT	0.72 (13.7)	0.64 (12.1)	<LoD	119.9 (16.6)	80.9 (12.6)	392.2 (15.6)	0.8 (25.1)

Reference proteins according to Zhang et al. [41]:
– Neurons, astrocytes, endothelial cells express ATP1A1.
– Both astrocytes and endothelial cells express ATP1A2, but endothelial cells in very low amounts.
– Neurons express ATP1A3.
– Astrocytes express GFAP.
The concentrations of different markers are not different between the samples and thus show the homogeneity of their cell composition. Therefore, the concentrations of ABCB1 proteins in the samples can be compared with each other. The QuaSAR plugin (Mani et al. [42]) was used to calculate the limit of detection and limit of quantitation.
CV (%) – biological and experimental variability, LoQ – lower limit of quantitation, LoD – lower limit of detection

(SpeedMill, AnalytikJena, Germany). Twenty millgrams of homogenate was mixed with homogenization buffer (20 mM EDTA, 140 mM NaCl, 5% SDS, cOmplete® mini protease inhibitor [Roche]) and incubated at 50 °C for 1 h [32]. After centrifugation at 13,000 rpm (30 min, 20 °C), protein concentration was determined using a BCA protein assay kit (ThermoFisher Scientific, USA). Samples were diluted to a protein concentration of 3 μg/μL in Laemmli buffer and denaturated at 42 °C for 30 min. Sixty milligrams of protein was loaded onto 12.5% TGX gels (Biorad, Germany) for electrophoresis and transferred onto 0.22 μm PVDF membranes using a TransBlot Turbo (Biorad, Germany). Membranes were blocked with 1.5% non-fat dry milk powder solubilized in PBS (0.01% Tween20) for 1 h at room temperature. Primary antibody was incubated over night at 4 °C, and secondary antibody incubation was 1 h at room temperature. Antibodies used were anti-ABCB1 (1:100, D-11, SantaCruz Biotechnologies), anti-β-Tubulin (1:10.000, SDL.3D10, Novus Biologicals), and anti-mouse HRP (1:10.000, NordicBiosite). Bands were detected using Clarity® Western ECL substrate (Biorad, Germany) and the Octoplus QPLEX imager (NHDyeAgnostics, Germany). Data analyzes were performed using Image Studio Lite (LI-COR Biosciences, Germany) and Microsoft Excel.

Sequencing. Genomic DNA of a hABCB1 mouse was purified using an innuPREP DNA Mini Kit (AnalytikJena AG, Germany). The humanized genomic locus was amplified in 25 μL reactions using TaKaRa LA TaqDNA Polymerase (TaKaRa Bio USA Inc.) according to manufacturer recommendations using 0.4 μM of each primer and an annealing temperature of 60 °C, resulting to single-banded PCR products. After amplification, the remaining primers and dNTPs were digested. The amplified fragments were sequenced using the Sanger process utilizing a primer walking strategy. For the sequencing of exons 3 and 4, PCR reactions were run with 12.5 ng template DNA in a total volume of 12.5 μL. PCR reactions including 0.3 μM of each PCR primer, 200 μM dNTPs, 1.5 mM $MgCl_2$ and 0.02 U/μL KAPA2G Robust polymerase. 35 cycles were run for each PCR with an initial denaturation step of 180 s at 95 °C followed by 35 cycles with a denaturation step for 20 s at 95 °C, an annealing step at 61 °C for 20 s, an elongation step for 100 s at 72 °C and a final elongation step at 72 ° for 45 s. Excess dNTPs and primers were removed from PCR reactions and Sanger sequencing was performed. All primers used are listed in Supplementary Table 1. Amplification, primer design, and sequencing were realized by Microsynth AG (Switzerland).

DNA Accessibility. Hotspots for DNA accessibility have been extracted from the ENCORE database. DNAse-seq data sets used were as follows: ENCSR337EDG, ENCSR179PIH, ENCSR358ESL, ENCSR469VGZ, ENCSR292QBA, and ENCSR767AJS. ATAC-seq data from ENCFF386CJN. Chromatin immunoprecipitation sequencing (ChIP-seq) data were extracted from ENCBS139ENC.

Data Availability. The data sets generated during and analyzed during the current study are available on reasonable request. Correspondence and requests for materials should be addressed to M.K. (markus.krohn@medisin.uio.no), J.P. (jens.pahnke@medisin.uio.no), W.L. (wolfgang.loescher@tiho-hannover.de), or O.L. (oliver.langer@ait.ac.at). All ENCODE data sets are publicly available at www.encodeproject.org.

Results

The humanized ABCB1 (hABCB1) strain under investigation was an unsolicited development by genOway (Lyon, France). The company used a strategy it claimed to have successfully employed earlier to introduce a canine *ABCB1* gene into the murine *Abcb1a* locus [33, 34]. To generate the hABCB1 strain, the mouse *Abcb1a* gene was humanized by introduction of the human *ABCB1* CDS into the gene's ATG start codon in exon 2. The mouse *Abcb1b* gene was partially deleted by insertion of a hygromycin cassette replacing exons 3 and 4 to ensure that only the human gene would be expressed. At purchase from genOway, the promising information available was that the human *ABCB1* mRNA is expressed at similar levels as is *Abcb1a* in wild-type animals in the tissues tested (brain, liver, intestine, kidney). Correct integration of the transgene had been checked using Southern blot. However, the knockout capability genOway aimed to introduce by gene floxing was reported to be non-functional and no protein expression data had been ascertained either. Thus, we agreed to verify the usefulness of this model in more detail and analyze ABCB1 transport activity/functionality and expression in the brain.

Positron Emission Tomography (PET) Imaging. The most important measure of validity for humanized ABC transporter mouse models is the functionality of the transporters in vivo. As transporter functionality is not assessable through mRNA or protein expression levels, we assessed ABCB1 transport activity at the BBB by PET imaging using the validated ABCB1 substrate radiotracer (*R*)-[^{11}C]verapamil in combination with administration of the ABCB1 inhibitor Tariquidar as described before [35, 36]. The hABCB1 strain from Taconic was included here, because it was extensively investigated before and shown to be insufficient for studies regarding ABCB1 function [21]. In vehicle-treated animals, brain uptake of (*R*)-[^{11}C]verapamil expressed as the brain-to-blood radioactivity concentration ratio at 60 min after radiotracer injection ($K_{b,brain}$) was significantly higher in hABCB1 mice from genOway ($K_{b,brain}$ = 3.26 ± 0.13) and Taconic ($K_{b,brain}$ = 2.76 ± 0.56) as compared with C57BL/6 mice ($K_{b,brain}$ = 1.22 ± 0.06, $p < 0.001$, 2-way ANOVA with Bonferroni *post-hoc* test, Figure 1). Tariquidar treatment significantly increased ($p < 0.05$, Student's *t* test) $K_{b,brain}$ in

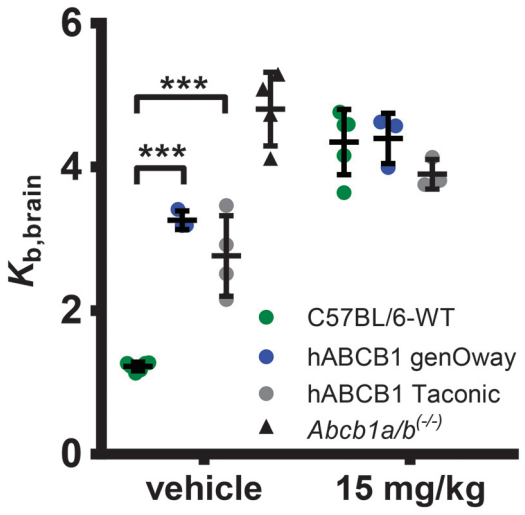

Figure 1. ABCB1 transport activity at the BBB measured with (*R*)-[^{11}C]verapamil PET imaging. Brain uptake of (*R*)-[^{11}C]verapamil expressed as brain-to-blood radioactivity concentration ratio ($K_{b,brain}$) at 60 min after radiotracer injection in female C57BL/6 mice (veh: n = 6, tariquidar: n = 5), hABCB1 mice (genOway; veh: n = 3, tariquidar: n = 3), and hABCB1 mice (Taconic; veh: n = 4, tariquidar: n = 3) treated with vehicle solution (2.5% [w/v] aq. dextrose solution) or tariquidar (15 mg/kg body weight) at 2 h before radiotracer injection. For comparison, $K_{b,brain}$ in vehicle-treated *Abcb1a/b*$^{(-/-)}$ mice (n = 4) is also shown [36]. Data are mean ± standard deviation. Statistical significance was determined by 2-way ANOVA with Bonferroni post-hoc test. **$p < 0.01$; ***$p < 0.001$

C57BL/6 mice by 3.6-fold ($K_{b,brain}$ = 4.35 ± 0.45), whereas increases were only 1.4-fold in hABCB1 mice from both genOway ($K_{b,brain}$ = 4.40 ± 0.35) and Taconic ($K_{b,brain}$ = 3.90 ± 0.21), respectively. For comparison, previously published $K_{b,brain}$ in vehicle-treated *Abcb1a/b* knockout mice (*Abcb1a/b*$^{(-/-)}$ mice) in C57BL/6 background was 4.81 ± 0.51 [36]. Although both humanized strains show some remaining transport capacity, as seen by the increase in $K_{b,brain}$ after tariquidar treatment, we concluded that the hABCB1 mice from genOway display the same lack of functionality as does the Taconic strain.

mRNA Expression Analyses. To reveal the cause for this lack of functionality, we rechecked human *ABCB1* and *Abcb1a* brain expression in the mice developed by genOway. The cycle threshold (ct) values of the amplification plots did not show a difference between mice of different age and were combined into one group for each strain. Target amplification could be verified for *Actb* (as endogenous reference) and *Abcb1a* mRNA in each sample, whereas *ABCB1* mRNA expression was only detected in humanized mice. Unexpectedly, mRNA expression of *Abcb1a* was still apparent at wild-type levels ($5.0 \times 10^{-3} \pm 2.4 \times 10^{-3}$) in hABCB1 mice ($4.0 \times 10^{-3} \pm 9.9 \times 10^{-4}$) (Figure 2). At the same time, *Abcb1a* mRNA levels in *ABCB1* humanized mouse brains were 35.9 times higher than human *ABCB1* expression ($4.0 \times 10^{-3} \pm 9.9 \times 10^{-4}$ vs. $1.1 \times 10^{-4} \pm 7.7 \times 10^{-5}$, one-way ANOVA, Tukey's honest significant difference post-hoc test, $p < 0.0001$, Figure 2).

mRNA expression analysis is sensitive to the position of primers and probes chosen. In this case, the primer set chosen for the *Abcb1a* mRNA was located over exon boundary 20–21, far distal to the introduced gene, because it covers all known splice variants of the gene. Thus, the qPCR outcome could result from the amplification of a greatly truncated *Abcb1a* mRNA that does not give rise to a functional protein. We performed an in silico translation starting from the first base of exon 3 to find possible open reading frames and see whether any truncated versions of ABCB1A proteins could be expressed in the humanized mice. As shown in Supplementary Figure 1, in frame 2 of exon 3, the last codon is an ATG which could initiate an open reading frame for a protein of 1239 amino acids length which would be fully identical to ABCB1A except for an N-terminal truncation of 37 amino acids. While this protein might still be functional, probably none of other 24 possible variants would (Supplementary Figure 1). Thus, we analyzed *Abcb1a* mRNA expression using two other assays located at exon boundaries 3–4 and 9–10, respectively, to verify the abundance of longer *Abcb1a* transcript variants. Figure 3 shows that the level of expression for all analyzed positions is similar between wild-type and hABCB1 mice. Resequencing of the engineered *Abcb1a* locus (see following section) confirmed the presence of valid loxP sites flanking the human *ABCB1* CDS. We sought to assess if these are not functional as has been stated by genOway. To do so, we crossed hABCB1 mice to a Cre-deleter mouse strain (CMV-driven Cre recombinase, see Section 0 for details) to check Cre recombination. Genotyping PCR confirmed that this crossing resulted in recombination of the locus and generation of genomic *ABCB1* knockout mice (referred to as human *ABCB1*$^{-/-}$ mice). However, as can be seen in Figure 3, Cre recombination had no effect on the *Abcb1a* mRNA expression level as assessed by any of the assays when compared to hABCB1 and wild-type mice. mRNA of the hABCB1 transgene was undetectable in these ABCB1$^{-/-}$ mice (not shown). Upon further communication, genOway revealed that only human *ABCB1* mRNA expression had been analyzed in-house, but not mouse gene expression. This fact might explain why the lack of functionality has not been detected earlier.

Protein Expression Analyses. Due to the unavailability of species-specific antibodies that allow differentiation between human and mouse ABCB1 proteins, we investigated protein expression of mouse ABCB1A/B and human ABCB1 using quantitative targeted absolute proteomics (QTAP) [26]. By detection of tryptic peptides specific for either the mouse or human protein variant, this method allows quantification of the transporters in whole brain homogenates. Table 1 shows that in wild-type mice both the peptide specific for mouse ABCB1A and the mouse ABCB1A/B-co-specific peptide are readily detectable. Although no ABCB1B-specific peptide has been analyzed, it can be assumed that most peptides found originate from ABCB1A proteins only, since both mouse specific peptides were found at similar quantities. In contrast, in hABCB1 mouse brains, no ABCB1A/B could be detected. Moreover, the human ABCB1 protein amount was below the lower limit of quantification (LoQ). These data are well in line with functional PET imaging data but seem to contradict qPCR results.

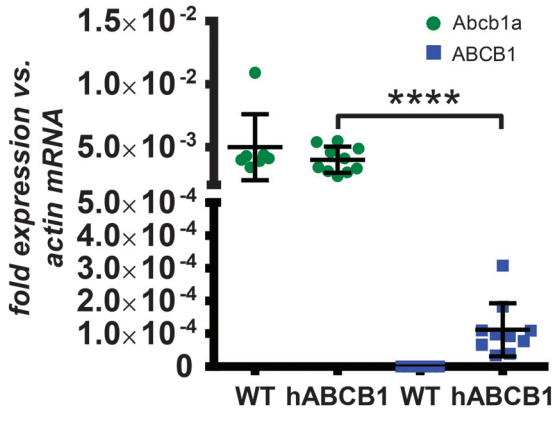

Figure 2. Relative mRNA expression of *Abcb1a* and *ABCB1*. Human *ABCB1* mRNA is expressed at very low levels in hABCB1 mice only. No decrease of *Abcb1a* mRNA expression was detected in hABCB1 mice compared to wild-type animals. Shown are the relative expression of mouse *Abcb1a* (green) and human *ABCB1* (blue) mRNA in male wild-type (n = 7) and hABCB1 (n = 10) mice based on the comparison of ct values. Ct values were normalized to mouse *Actb* mRNA expression using $2^{(-\Delta ct)}$ calculation. Data are mean ± standard deviation. Statistical significance was determined by 1-way ANOVA with Tukey's honest significant difference post-hoc test. ****$p < 0.0001$

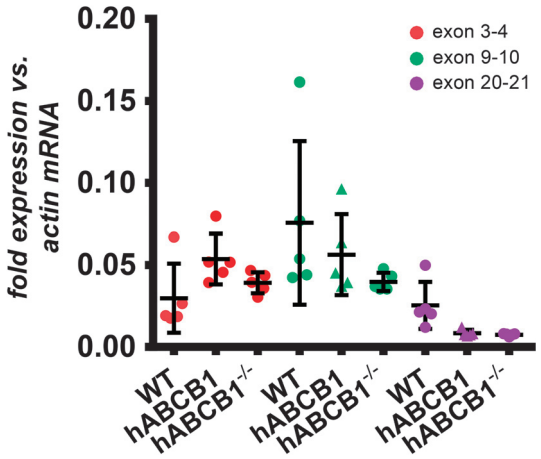

Figure 3. Exon junction-specific mRNA expression of *Abcb1a*. Abundance of *Abcb1a* mRNAs with different lengths was assessed using assays covering the indicated exon junctions in female wild-type mice (n = 5), hABCB1 mice (n = 5), as well as in hABCB1 mice (n = 5) crossed to a Cre-deleter mouse strain (human *ABCB1*$^{-/-}$). No differential expression between strains was found within each assay location. Data are mean ± standard deviation. Statistical significance was determined by 1-way ANOVA with Tukey's honest significant difference post-hoc test, significance level $p < 0.05$

However, it is known that mRNA expression data do often not correlate well with protein expression data. Most interestingly, human *ABCB1*$^{-/-}$ mice displayed partly rescued ABCB1A protein expression. However, also with this method, we were not able to determine the extent of the N-terminal truncation that was inflicted by Cre recombination of the *Abcb1a* locus. Western blot analyses using a C-terminal targeting antibody additionally supported our PET imaging data; however, no obvious protein truncation could be detected (Supplementary Figure 2).

Genomic DNA Sequencing. We sought to find possible explanations for the revealed shortcomings and to gather knowledge for a more successful knock-in strategy by sequencing of the humanized genomic locus. The sequenced region comprised 6089 bp including segments of mouse genomic DNA at both the 5′- and 3′-ends, suggesting that the engineered locus has been covered in full. As indicated in Figure 4, the human CDS including its 3′-untranslated region (UTR), but without the 5′-UTR, was successfully fused to the start codon of the *Abcb1a* gene located in exon 2. Exon 2 of *Abcb1a* was deleted except for its untranslated base pairs -1 to -6 from transcription start site (TSS). At TSS +4598 bp, the unaltered mouse genomic DNA sequence starts again with the first base pair aligning to intronic base pair TSS +267 of the mouse *Abcb1a* gene in wild-type mice (Supplementary Figure 3). Thus, exon 2 (TSS 0 to +65) and the first 202 bp of intron 2 have been deleted by the human CDS construct, in total 268 bp. Additional sequencing of exons 3 and 4 revealed that neither exon 3 nor exon 4 has been deleted nor altered during gene targeting, a fact later confirmed by genOway (Supplementary Figure 4). These data corroborate the mRNA expression analyses and again imply the possibility of expression of a truncated ABCB1A protein that is, however, most probably dysfunctional.

Unexpectedly, in addition to the loxP sites flanking the hABCB1 gene, we found DNA of unknown origin flanking both sites. In case of the 5′-loxP site, there are 20 bp upstream and 17 bp downstream of the actual Cre recombinase recognition motif. The 3′-loxP site is flanked by 76 bp and 23 bp, respectively. BLAST results strongly suggest remnants of cloning vectors containing loxP sites. The alien DNA containing the 5′-loxP site is situated −413 bp to −492 bp from TSS, thereby disrupting intron 1 of *Abcb1a* and possibly interfering with promoter elements.

Thus, we searched the ENCODE database for information about DNA accessibility of this region [37, 38]. Several DNAse-seq (DNase I hypersensitive sites sequencing) data sets (deposited after generation of this mouse model) derived from adult mouse brains revealed hotspots in the region of interest. The combined hotspot region (covered by at least 5 data sets) reaches from about 200 bp upstream of exon 1 until about 160 bp downstream of exon 2 (Figure 5). ATAC-seq (Assay for Transposase-Accessible Chromatin sequencing) data generated from postnatal mouse forebrains revealed a hotspot of about 690 bp reaching until exon 2 (Figure 5). Furthermore, ChIP-seq experiments targeting tri-methylated histone H3 (H3K4me3) found a similar hotspot in cortical plate samples of adult mice (Figure 5). Due to the repeated occurrence of high DNA accessibility using different methods, we conclude that a region of high regulatory importance includes at least intron 1 of *Abcb1a* but most likely exon 2 as well.

Discussion

With the study presented here, we set out to assess the functionality and expression of human ABCB1 protein in the brain of

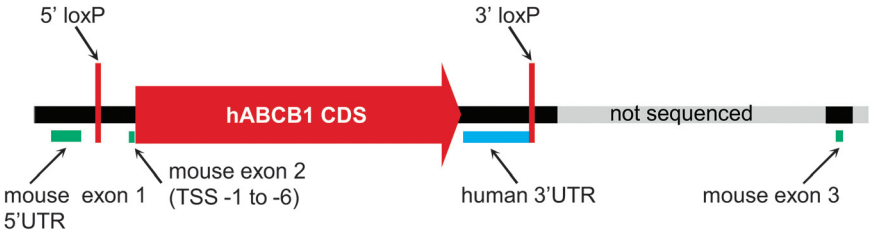

Figure 4. Depiction of the humanized *Abcb1a* gene locus. Shown are the sequenced region (6089 bp, black) and the downstream adjacent mouse sequence not included in the sequencing (light grey). The human *ABCB1* CDS was fused into the TSS, which left the untranslated base pairs TSS -1 to -6 of exon 2 behind (green). *ABCB1* CDS has been introduced with its 3′UTR and additional 45 bp of human genomic downstream sequence. At the 3′ transition towards the mouse genomic sequence, a loxP site has been introduced which is flanked by altogether 99 bp of unknown origin. The same is true for the 5′ situated loxP site, which is flanked by additional 37 bp, respectively, and inserted into intron 1 of mouse *Abcb1a*. The picture is not proportional to the genomic arrangement.

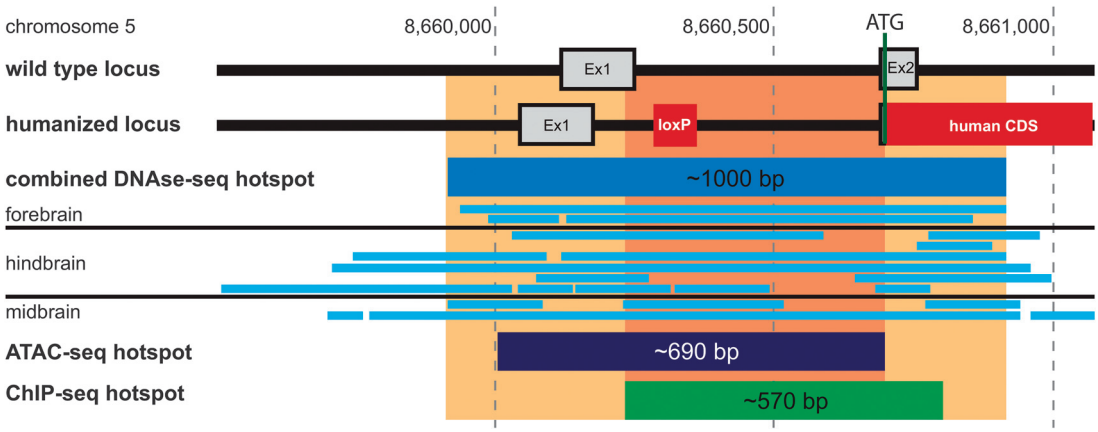

Figure 5. *Abcb1a* promoter region analysis. Shown are the *Abcb1a* loci of wild-type and hABCB1 mice in comparison. ENCODE database searches revealed the indicated hotspots of open/accessible chromatin found in mouse brains using DNAse-seq, ATAC-seq, and ChIP-seq methods. The area of highest density of overlapping hotspots (orange/light orange) covers more than 200 bp indicating the importance of this region for *Abcb1a* gene expression.

an *Abcb1a* humanized, *Abcb1b* knockout mouse model [21] developed by genOway. Sequence analyses of the humanized locus confirmed proper insertion and targeting of the mouse *Abcb1a* gene including the deletion of mouse exon 2. Nevertheless, mRNA expression data revealed a very low expression of *ABCB1* mRNA at a level less than 3% of that of *Abcb1a* in wild-type mice (Figure 2). Accordingly, human ABCB1 protein did not reach the lower limit of quantitation and functional PET analyses revealed a knockout phenotype of hABCB1 mice. Whereas (*R*)-[^{11}C]verapamil PET imaging without tariquidar treatment led to significantly higher radioactivity uptake in the brains of hABCB1 mice as compared to wild-type mice, ABCB1 inhibition with tariquidar induced only a minor increase in radioactivity uptake in hABCB1 animals. Hence, the genOway hABCB1 mice display a functional phenotype very similar to that of hABCB1 mice introduced by Taconic (see also Sadiq et al. [21]).

Intriguingly, murine *Abcb1a* mRNA is still present at wild-type levels in the humanized mice's brain (Figure 2) indicating the expression of a truncated *Abcb1a* gene product starting downstream of exon 2. In silico translation analysis of the *Abcb1a* coding sequence and qPCR revealed the possibility of a protein being expressed that lacks at least the first 37 amino acids and thus the cytoplasmic N-terminus up to transmembrane helix 1 (Figure 3). However, mouse ABCB1A/B proteins were not detectable at all in hABCB1 mice (Table 1).

Since the human CDS has been inserted correctly and this strategy was employed successfully to introduce a canine *ABCB1* earlier [33, 34], the main question is: what caused the lack of expression in both (Taconic and genOway) humanized mouse models? A review of the canine *ABCB1* mouse data points to an answer. The major difference to both humanized strains is the insertion of a mutated *ABCB1* CDS in the canine model. Especially, dogs of the Collie lineage often suffer from severe adverse responses to ivermectin, which is a commonly used anthelmintic [39]. It is also that substrate of ABCB1 and genetic analyses of ivermectin-sensitive Collies revealed an exonic deletion of 4 bps leading to a frameshift and premature termination of translation [40]. The canine *ABCB1* mouse strain was developed as an alternative model to Collies in the search for anthelmintic drugs that do not pose a life danger to such dogs. The canine *ABCB1* mouse strain, therefore, is functionally an *ABCB1*-knockout model in which a lack of expression of the canine ABCB1 protein cannot be detected using drug-induced phenotypes or PET measurements. Thus, it is very likely that the canine *ABCB1* mice exhibit a similar lack of protein expression as observed in the human *ABCB1* strains developed by Taconic and genOway (see Table 2 for comparison).

Notably, all strains have been designed using insertion of *ABCB1* CDS into the ATG start codon of *Abcb1a*. Sadiq et al. [21] found the human ABCB1 protein expression in brain capillaries of hABCB1 mice from Taconic to be about 1.5% of that of ABCB1A in wild-type mice. Interestingly, the Taconic hABCB1 mice still expressed mouse ABCB1A protein, though at a level of only about 10% of that of wild-type mice [21]. In the genOway strain, ABCB1A/B protein levels in hABCB1 mice did not reach the lower limit of detection. This difference is most probably due to the different modes of tissue preparation used in both studies. While Sadiq et al. analyzed capillary-enriched brain preparations only, we used whole brain homogenates. Although detection of any ABCB1 protein in whole brain homogenates is hampered by a low enrichment of microvessels, ABCB1A was readily detectable in wild-type mice (Table 1). Unfortunately, the LoQ of human ABCB1 was rather high compared to the murine variants (0.7 vs. 0.23 fmol/μg protein). Nevertheless, human ABCB1 protein was at least detectable in hABCB1 mice whereas ABCB1A was not despite its much lower LoD (0.23 vs. 0.08 fmol/μg protein). We therefore conclude that the residual increase of $K_{b,brain}$ in hABCB1 mice seen after tariquidar treatment is the result of a very low expression of human ABCB1 only.

More importantly, the combined data from our study and from Sadiq et al. show that especially the disruption of exon 2 of *Abcb1a* diminishes expression of the inserted gene/protein. Only the ABCB1 humanized mice developed by genOway possess a known alteration of intron 1, but neither the hABCB1 mice from Taconic nor the canine ABCB1 mice, suggesting that the structural integrity of exon 2 is of paramount importance since all models lack protein expression. The overlap of several hotspots of DNA accessibility extracted from ENCODE data sets within the region of CDS insertion reinforces its importance in gene regulation. Interestingly, the lack of two-thirds of intron 1 and all of exon 2 in human *ABCB1*$^{-/-}$ mice restored mouse ABCB1A protein expression to about 50% of wild-type levels according to QTAP results. However, Western blot results corroborate PET imaging data and QTAP results but, confusingly, do not reveal truncated protein variants. The lack of a visible shift in protein size might be due to the extremely weak signals though and a lack of resolution of the chosen gel matrix.

One could speculate that recombination of the locus restores some regulatory features partly located in intron 2 that have been disrupted by insertion of the CDS. More likely, however, it seems that alternative splicing and/or alternative polyadenylation occurs, which leads to truncated/unstable mRNAs and low translation yields. Nevertheless, the somewhat sloppy integration of the loxP sites might have had an additional effect on gene expression.

In conclusion, we think a humanization of the *Abcb1a* gene would have a higher likelihood of success when the human CDS is being inserted into exon 3 while intron 1/exon 2 is left untouched or introduced changes kept to a minimum. Exon 2 encodes for the first 21 aa of ABCB1A which share only 52.2% identity to human ABCB1. Hence, insertion of the human CDS into exon 3 without adapting exon 2 would generate a chimeric hABCB1 model. The same strategy was recently successfully employed to develop humanized *ABCC1* and humanized *ABCA7* mice (Krohn et al., unpublished). On the other hand, humanization of the first 21 aa could be achieved by exchanging 13 of the 68 bp of exon 2 plus an additional insertion of one codon. Thus, this decision might become a trade-off between protein expression and protein function. Although the functional relevance of this very N-terminus remains to be determined, it seems unlikely to have much impact on substrate affinities which is the most important issue. To our knowledge, in this region, no single nucleotide polymorphisms (SNPs) or

Table 2. ABCB1 knock-in mouse model comparison

Model	Producer	Insertion site	Insertion	Special features	Ref
Canine ABCB1	genOway	*Abcb1a* ATP-start codon	Canine cDNA (~4300 bp)	Intended 4 bp deletion with frame shift at pos. TSS +294	[33]
Humanized ABCB1	Taconic	*Abcb1a* ATP-start codon	Human cDNA (~4300 bp)	*Abcb1b* knockout	[21]
Humanized ABCB1	genOway	*Abcb1a* ATP-start codon	Human cDNA (5106 bp)	loxP insertion TSS −492 and TSS +4628	This work

Overview of ABCB1 knock-in mouse models published to date with insertions site of the alien DNA and distinctive features. None of the models express functional ABCB1 proteins.

mutations of clinical relevance are known for any ABC transporter. In addition, the use of a codon usage optimized CDS should aid expression levels. We therefore suggest that the approach of choice should be a chimeric hABCB1 mouse strain that will most likely retain the original level and pattern of protein expression.

Funding Sources

This work was supported by grants from the Deutsche Forschungsgesellschaft (DFG) to J.P. (grant number: DFG PA930/9-1) and W.L. (grant number: DFG LO274/16-1), the Austrian Science Fund (FWF) (grant number: I 1609-B24 to O.L.), and the Lower Austria Corporation for Research and Education (NFB) (grant number: LS14-008 [T. Wanek]; LS15-003 [O. Langer]). The work of J.P. was also financed by the following grants: Deutsche Forschungsgemeinschaft/Germany (DFG PA930/12-1); Leibniz Society/Germany (SAW-2015-IPB-2); HelseSØ/Norway (2016062); Norsk forskningsrådet/Norway (246392, 247179 [NeuroGeM], 248772, 251290, 260786 [PROP-AD]); Horizon 2020/European Union (643417 [PROP-AD]). NeuroGeM is an EU Joint Programme — Neurodegenerative Disease Research (JPND) project. The project is supported through the following funding organisations under the aegis of JPND — www.jpnd.eu (CIHR — Canada, BMBF — Germany, NRF no. 247179 — Norway, ZonMW — The Netherlands). PROP-AD is an EU Joint Programme — Neurodegenerative Disease Research (JPND) project. The project is supported through the following funding organisations under the aegis of JPND — www.jpnd.eu (AKA no. 301228 — Finland, BMBF no. 01ED1605 — Germany, CSO-MOH no. 30000-12631 — Israel, NFR no. 260786 — Norway, SRC no. 2015-06795 — Sweden). This project has received funding from the European Union's Horizon 2020 research and innovation programme under grant agreement no. 643417 (JPco-fuND).

Authors' Contributions

M.K., O.L., W.L., and J.P. planned the study. M.K. and A.N. performed the qPCR. T.W. and O.L. performed the PET analyses and prepared Figure 1. M.-C.M. and X.D. performed the QTAP. M.K. analyzed the sequencing and ENCODE data. M.K. wrote the article and prepared the figures. All authors discussed the results and commented on the article.

Conflict of Interest

The authors have no conflict of interest to report.

Acknowledgments. The authors thank Sandra Noack, Ivan Eiriz Delgado, David Gomez-Zepeda, Meryam Taghi, Wang-Qing Liu, Cerina Chhuon, Michel Vidal, and Ida-Chiara Guerrera for their assistance. They also thank genOway S.A. for their openness in discussing the findings and all members of the ENCODE Consortium and Portal for providing the valuable data sets.

References

1. Kis O, Robillard K, Chan GN, Bendayan R. The complexities of antiretroviral drug–drug interactions: role of ABC and SLC transporters. Trends Pharmacol Sci. 2010;31:22–35.

2. Marchetti S, Mazzanti R, Beijnen JH, Schellens JH. Concise review: clinical relevance of drug drug and herb drug interactions mediated by the ABC transporter ABCB1 (MDR1, P-glycoprotein). Oncologist. 2007;12:927–41.

3. The International Transporter Consortium, Giacomini KM, Huang SM, Tweedie DJ, Benet LZ, Brouwer KL, et al. Membrane transporters in drug development. Nat Rev Drug Discov. 2010;9:215–36.

4. Schumacher T, Krohn M, Hofrichter J, Lange C, Stenzel J, Steffen J, et al. ABC transporters B1, C1 and G2 differentially regulate neuroregeneration in mice. PLoS One. 2012;7:e35613.

5. Alison MR. Tissue-based stem cells: ABC transporter proteins take centre stage. J Pathol. 2003;200:547–50.

6. Islam MO, Kanemura Y, Tajria J, Mori H, Kobayashi S, Shofuda T, et al. Characterization of ABC transporter ABCB1 expressed in human neural stem/progenitor cells. FEBS Lett. 2005;579:3473–80.

7. Löscher W, Potschka H. Drug resistance in brain diseases and the role of drug efflux transporters. Nature reviews Neuroscience. 2005;6:591–602.

8. Cirrito JR, Deane R, Fagan AM, Spinner ML, Parsadanian M, Finn MB, et al. P-glycoprotein deficiency at the blood–brain barrier increases amyloid-beta deposition in an Alzheimer disease mouse model. J Clin Invest. 2005;115:3285–90.

9. Krohn M, Bracke A, Avchalumov Y, Schumacher T, Hofrichter J, Paarmann K, et al. Accumulation of murine amyloid-beta mimics early Alzheimer's disease. Brain. 2015;138:2370–82.

10. Pahnke J, Fröhlich C, Paarmann K, Krohn M, Bogdanovic N, Arsland D, et al. Cerebral ABC transporter-common mechanisms may modulate neurodegenerative diseases and depression in elderly subjects. Arch Med Res. 2014;45:738–43.

11. Krohn M, Lange C, Hofrichter J, Scheffler K, Stenzel J, Steffen J, et al. Cerebral amyloid-beta proteostasis is regulated by the membrane transport protein ABCC1 in mice. J Clin Invest. 2011;121:3924–31.

12. Yvan-Charvet L, Welch C, Pagler TA, Ranalletta M, Lamkanfi M, Han S, et al. Increased inflammatory gene expression in ABC transporter-deficient macrophages: free cholesterol accumulation, increased signaling via toll-like receptors, and neutrophil infiltration of atherosclerotic lesions. Circulation. 2008;118:1837–47.

13. Cole SP. Multidrug resistance protein 1 (MRP1, ABCC1), a "multitasking" ATP-binding cassette (ABC) transporter. J Biol Chem. 2014;289:30880–8.

14. Mason BL, Pariante CM, Thomas SA. A revised role for P-glycoprotein in the brain distribution of dexamethasone, cortisol, and corticosterone in wild-type and ABCB1A/B-deficient mice. Endocrinology. 2008;149:5244–53.

15. Yamazaki M, Neway WE, Ohe T, Chen I, Rowe JF, Hochman JH, et al. In vitro substrate identification studies for p-glycoprotein-mediated transport: species difference and predictability of in vivo results. J Pharmacol Exp Ther. 2001;296:723–35.

16. Baltes S, Gastens AM, Fedrowitz M, Potschka H, Kaever V, Löscher W. Differences in the transport of the antiepileptic drugs phenytoin, levetiracetam and carbamazepine by human and mouse P-glycoprotein. Neuropharmacology. 2007;52:333–46.

17. Feng B, Mills JB, Davidson RE, Mireles RJ, Janiszewski JS, Troutman MD, et al. In vitro P-glycoprotein assays to predict the in vivo interactions of P-glycoprotein with drugs in the central nervous system. Drug Metab Dispos. 2008;36:268–75.

18. Helms HC, Abbott NJ, Burek M, Cecchelli R, Couraud PO, Deli MA, et al. In vitro models of the blood–brain barrier: an overview of commonly used brain endothelial cell culture models and guidelines for their use. J Cereb Blood Flow Metab. 2016;36:862–90.

19. Devoy A, Bunton-Stasyshyn RK, Tybulewicz VL, Smith AJ, Fisher EM. Genomically humanized mice: technologies and promises. Nat Rev Genet. 2011;13:14–20.

20. Dallas S, Salphati L, Gomez-Zepeda D, Wanek T, Chen L, Chu X, et al. Generation and characterization of a breast cancer resistance protein humanized mouse model. Mol Pharmacol. 2016;89:492–504.

21. Sadiq MW, Uchida Y, Hoshi Y, Tachikawa M, Terasaki T, Hammarlund-Udenaes M. Validation of a P-glycoprotein (P-gp) humanized mouse model by integrating selective absolute quantification of human MDR1, Mouse Mdr1a and Mdr1b protein expressions with in vivo functional analysis for blood–brain barrier transport. PLoS One. 2015;10:e0118638.

22. Brunner M, Langer O, Sunder-Plassmann R, Dobrozemsky G, Müller U, Wadsak W, et al. Influence of functional haplotypes in the drug transporter gene ABCB1 on central nervous system drug distribution in humans. Clin Pharmacol Ther. 2005;78:182–90.

23. Loening AM, Gambhir SS. AMIDE: a free software tool for multimodality medical image analysis. Mol Imaging. 2003;2:131–7.

24. Ohtsuki S, Schaefer O, Kawakami H, Inoue T, Liehner S, Saito A, et al. Simultaneous absolute protein quantification of transporters, cytochromes P450, and UDP-glucuronosyltransferases as a novel approach for the characterization of individual human liver: comparison with mRNA levels and activities. Drug Metab Dispos. 2012;40:83–92.

25. Hoshi Y, Uchida Y, Tachikawa M, Inoue T, Ohtsuki S, Terasaki T. Quantitative atlas of blood–brain barrier transporters, receptors, and tight junction proteins in rats and common marmoset. J Pharm Sci. 2013;102:3343–55.

26. Uchida Y, Tachikawa M, Obuchi W, Hoshi Y, Tomioka Y, Ohtsuki S, et al. A study protocol for quantitative targeted absolute proteomics (QTAP) by LC–MS/MS: application for inter-strain differences in protein expression levels of transporters, receptors, claudin-5, and marker proteins at the blood–brain barrier in ddY, FVB, and C57BL/6J mice. Fluids Barriers CNS. 2013;10:21.

27. Chaves C, Gomez-Zepeda D, Auvity S, Menet MC, Crete D, Labat L, et al. Effect of subchronic intravenous morphine infusion and naloxone-precipitated morphine withdrawal on P-gp and Bcrp at the rat blood–brain barrier. J Pharm Sci. 2016;105:350–8.

28. Kamiie J, Ohtsuki S, Iwase R, Ohmine K, Katsukura Y, Yanai K, et al. Quantitative atlas of membrane transporter proteins: development and application of a highly sensitive simultaneous LC/MS/MS method combined with novel in-silico peptide selection criteria. Pharm Res. 2008;25:1469–83.

29. Gomez-Zepeda D, Chaves C, Taghi M, Sergent P, Liu WQ, Chhuon C, et al. Targeted unlabeled multiple reaction monitoring analysis of cell markers for the study of sample heterogeneity in isolated rat brain cortical microvessels. J Neurochem. 2017;142:597–609.

30. Maclean B, Tomazela DM, Abbatiello SE, Zhang S, Whiteaker JR, Paulovich AG, et al. Effect of collision energy optimization on the measurement of

peptides by selected reaction monitoring (SRM) mass spectrometry. Anal Chem. 2010;82:10116–24.

31. MacLean B, Tomazela DM, Shulman N, Chambers M, Finney GL, Frewen B, et al. Skyline: an open source document editor for creating and analyzing targeted proteomics experiments. Bioinformatics. 2010;26:966–8.

32. Kopec AM, Rivera PD, Lacagnina MJ, Hanamsagar R, Bilbo SD. Optimized solubilization of TRIzol-precipitated protein permits Western blotting analysis to maximize data available from brain tissue. J Neurosci Methods. 2017;280:64–76.

33. Swain MD, Orzechowski KL, Swaim HL, Jones YL, Robl MG, Tinaza CA, et al. P-gp substrate-induced neurotoxicity in an Abcb1a knock-in/Abcb1b knock-out mouse model with a mutated canine ABCB1 targeted insertion. Res Vet Sci. 2013;94:656–61.

34. Orzechowski KL, Swain MD, Robl MG, Tinaza CA, Swaim HL, Jones YL, et al. Neurotoxic effects of ivermectin administration in genetically engineered mice with targeted insertion of the mutated canine ABCB1 gene. Am J Vet Res. 2012;73:1477–84.

35. Römermann K, Wanek T, Bankstahl M, Bankstahl JP, Fedrowitz M, Müller M, et al. (R)-[^{11}C]verapamil is selectively transported by murine and human P-glycoprotein at the blood–brain barrier, and not by MRP1 and BCRP. Nucl Med Biol. 2013;40:873–8.

36. Wanek T, Römermann K, Mairinger S, Stanek J, Sauberer M, Filip T, et al. Factors governing P-glycoprotein-mediated drug–drug interactions at the blood–brain barrier measured with positron emission tomography. Mol Pharmaceutics. 2015;12:3214–25.

37. Consortium EP. An integrated encyclopedia of DNA elements in the human genome. Nature. 2012;489:57–74.

38. Sloan CA, Chan ET, Davidson JM, Malladi VS, Strattan JS, Hitz BC, et al. ENCODE data at the ENCODE portal. Nucleic Acids Res. 2016;44:D726–32.

39. Mealey KL. Therapeutic implications of the MDR-1 gene. J Vet Pharmacol Ther. 2004;27:257–64.

40. Mealey KL, Bentjen SA, Gay JM, Cantor GH. Ivermectin sensitivity in collies is associated with a deletion mutation of the mdr1 gene. Pharmacogenetics. 2001;11:727–33.

Supporting information

Supplementary Figure 1. Full exonic sequence of *Abcb1a*.

acagtggaacagcggtttccaggagctgctggtcccatcttccaaggctctgctcaactcagagccgc
ttcttccaaagtctacatcttggtggactttgcagaggaaaccgggaggtagagacacgtgag|gtcg
tgATGGAACTTGAAGAGGACCTTAAGGGAAGAGCAGACAAGAACTTCTCAAAGATGGGCAAAAAGAG|
TAAAAAGGAGAAGAAAGAAAAGAAACCAGCAGTCAGTGTGCTTACAATG|TTTCGTTATGCAGGTTGG
CTGGACAGGTTGTACATGCTGGTGGGAACTCTGGCTGCTATTATCCATGGAGTGGCGCTCCCACTTAT
GATGCTGATCTTTGGTGACATGACAGATAGCTTTGCAAGTGTAGGAAACGTCTCTAAAAACAGTACTA
ATATGA|GTGAGGCCGATAAAAGAGCCATGTTTGCCAAACTGGAGGAAGAAATGACCAC|GTACGCCT
ACTATTACACCGGGATTGGTGCTGGTGTGCTCATAGTTGCCTACATCCAGGTTTCATTTTGGTGCCTG
GCAGCTGGAAGACAGATACACAAGATCAGGCAGAAGTTTTTTCATGCTATAATGAATCAGGAGATAGG
CTGGTTTGATGTGCATGACGTTGGGGAGCTCAACACCCGGCTCACAGA|TGATGTTTCCAAAATTAAT
GAAGGAATTGGTGACAAAATCGGAATGTTCTTCCAGGCAATGGCAACATTTTTTGGTGGTTTTATAAT
AGGATTTACCCGTGGCTGGAAGCTAACCCTTGTGATTTTGGCCATCAGCCCTGTTCTTGGACTGTCAG
CTGGTATTTGGGCAAAG|ATATTGTCTTCATTTACTGATAAGGAACTCCATGCTTATGCAAAAGCTGG
AGCAGTTGCTGAAGAAGTCTTAGCAGCCATCAGAACTGTGATTGCGTTTGGAGGACAAAAGAAGGAAC
TTGAAAG|GTACAATAACAACTTGGAAGAAGCTAAAAGGCTGGGGATAAAGAAAGCTATCACGGCCAA
CATCTCCATGGGTGCAGCTTTTCTCCTTATCTATGCATCATATGCTCTGGCATTCTGGTATGGGACTT
CCTTGGTCATCTCCAAAGAATACTCTATTGGACAAGTGCTCACT|GTCTTCTTTTCCGTGTTAATTGG
AGCATTCAGTGTTGGACAGGCATCTCCAAATATTGAAGCCTTCGCCAATGCACGAGGAGCAGCTTATG
AAGTCTTCAAAATAATTGATAAT|AAGCCCAGTATAGACAGCTTCTCAAAGAGTGGGCACAAACCAGA
CAACATACAAGGAAATCTGGAATTTAAGAATATTCACTTCAGTTACCCATCTCGAAAAGAAGTTCAG|
ATCTTGAAGGGCCTCAATCTGAAGGTGAAGAGCGGACAGACGGTGGCCCTGGTTGGCAACAGTGGCTG
TGGAAAAAGCACAACTGTCCAGCTGATGCAAAGGCTCTACGACCCCCTAGATGGCATG|GTCAGTATC
GACGGACAGGACATCAGAACCATCAATGTGAGGTATCTGAGGGAGATCATTGGTGTGGTGAGTCAGGA
ACCTGTGCTGTTTGCCACCACGATCGCCGAGAACATTCGCTATGGCCGAGAAGATGTCACCATGGATG
AGATTGAGAAAGCTGTCAAGGAAGCCAATGCCTATGACTTCATCATGAAACTGCCCCAC|CAATTTGA
CACCCTGGTTGGTGAGAGAGGGGCGCAGCTGAGTGGGGGACAGAAACAGAGAATCGCCATTGCCCGGG
CCCTGGTCCGCAATCCCAAGATCCTTTTGTTGGACGAGGCCACCTCAGCCCTGGATACAGAAAGTGAA
GCTGTGGTTCAGGCCGCACTGGATAAG|GCTAGAGAAGGCCGGACCACCATTGTGATAGCTCATCGCT
TGTCTACCGTTCGTAATGCTGACGTCATTGCTGGTTTTGATGGTGGTGTCATTGTGGAGCAAGGAAAT
CATGATGAGCTCATGAGAGAAAAGGGCATTTACTTCAAACTTGTCATGACACAG|ACAGCAGGAAATG
AAATTGAATTAGGAAATGAAGCTTGTAAATCTAAGGATGAAATTGATAATTTAGACATGTCTTCAAAA
GATTCAGGATCCAGTCTAATAAGAAGAAGATCAACTCGCAAAAGCATCTGTGGACCACATGACCAAGA
CAGGAAGCTTAGTACCAAAGAGGCCCTG|GATGAAGATGTACCTCCAGCTTCCTTTTGGCGGATCCTG
AAGTTGAATTCAACTGAATGGCCTTATTTTGTGGTTGGTATATTCTGTGCCATAATAAATGGAGGCTT
ACAGCCAGCATTCTCCGTAATATTTTCAAAAGTTGTAGGG|GTTTTTACAAATGGTGGCCCCCCTGAA
ACCCAGCGGCAGAACAGCAACTTGTTTTCCTTGTTGTTTCTGATCCTTGGGATCATTTCTTTCATTAC
ATTTTTTCTTCAG|GGCTTCACATTTGGCAAAGCTGGAGAGATCCTCACCAAGCGACTCCGATACATG
GTTTTCAAATCCATGCTGAGACAG|GATGTGAGCTGGTTTGATGACCCTAAAAACACCACCGGAGCAC
TGACCACCAGGCTCGCCAACGATGCTGCTCAAGTGAAAGGG|GCTACAGGGTCTAGGCTTGCTGTGAT
TTTCCAGAACATAGCAAATCTTGGGACAGGAATCATCATATCCCTAATCTATGGCTGGCAACTAACAC
TTTTACTCTTAGCAATTGTACCCATCATTGCGATAGCAGGAGTGGTTGAAATGAAAATGTTGTCTGGA
CAAGCACTGAAAGATAAGAAGGAACTAGAAGGTTCTGGAAAG|ATTGCTACGGAAGCAATTGAAAACT
TCCGCACTGTTGTCTCTTTGACTCGGGAGCAGAAGTTTGAAACCATGTATGCCCAGAGCTTGCAGATA
CCATACAG|AAATGCGATGAAGAAAGCACACGTGTTTGGGATCACGTTCTCCTTCACCCAGGCCATGA
TGTATTTTTCTTATGCTGCTTGTTTCCGGTTCGGTGCCTACTTGGTGACACAACAACTCATGACTTTT
GAAAATGTTCTGTT|AGTATTCTCAGCTATTGTCTTTGGTGCCATGGCAGTGGGGCAGGTCAGTTCAT
TCGCTCCTGACTATGCGAAAGCCACAGTGTCAGCATCCCACATCATCAGGATCATTGAGAAAACCCCC
GAGATTGACAGCTACAGCACGCAAGGCCTAAAGCCG|AATATGTTGGAAGGAAATGTGCAATTTAGTG
GAGTCGTGTTCAACTATCCCACCCGACCCAGCATCCCAGTGCTTCAGGGGCTGAGCCTTGAGGTGAAG
AAGGGCCAGACGCTGGCCCTGGTGGGCAGCAGTGGCTGCGGGAAGAGCACAGTGGTCCAGCTGCTCGA
GCGCTTCTACGACCCCATGGCTGGATCAGTG|TTTCTAGATGGCAAAGAAATAAAGCAACTGAATGTC

CAGTGGCTCCGAGCACAGCTGGGCATTGTGTCCCAAGAGCCCATTCTCTTTGACTGCAGCATCGCAGA
GAACATTGCCTACGGAGACAACAGCCGGGTCGTGTCTTATGAGGAGATTGTGAGGGCAGCCAAGGAGG
CCAACATCCACCAGTTCATCGACTCGCTACCTGAT|AAATACAACACCAGAGTAGGAGACAAAGGCAC
TCAGCTGTCGGGTGGGCAGAAGCAGCGCATCGCCATCGCACGCGCCCTCGTCAGACAGCCTCACATTT
TACTTCTGGACGAAGCAACATCAGCTCTGGATACAGAAAGTGAAAAG|GTTGTCCAGGAAGCGCTGGA
CAAAGCCAGGGAAGGCCGCACCTGCATTGTGATCGCTCACCGCCTGTCCACCATCCAGAACGCGGACT
TGATCGTGGTGATTCAGAACGGCAAGGTCAAGGAGCACGGCACCCACCAGCAGCTGCTGGCGCAGAAG
GGCATCTACTTCTCAATGGTCAGTGTGCAGGCTGGAGCAAAGCGCTCATGAactgtgaccatgtaaga
tgttaagtatttttattgtttgtattcatatatggtgtttaatccaagtcaaaaggaaaacacttact
aaaatagccagttatctatttttctgccacagtggaaagcatttagtttggtttagagtcttcagaggc
tttgtaattaaaaaaacaaaaatagatacagcatcaaatggagattaatgctttaaaatgcactataa
aatttataaaagggttaaaagtgaatgtttgataatatatacttttatttatactttctcatttgtaa
ctataactgatttctgcttaacaaattatgtatgtatcaaaaattactgaaatgtttgtataaagtat
atatagtgaaactgagcattcatatttttgagttattttgctcaaaatgcatgcgaaattatatattg
tcccaactggaatattgtacataattttagcctttaaaaaacagtccattactgggggggaggggcat
cactctatgggcaaagtgttactcagacatgggcacctgagttcagatccctaccacctaagtaagca
gcaaggtgtggtgtttttgtaatgccagtgctagaggcagaaacagacagatcctgcaggctcagtgg
ctggccaaacagcctagccaacatagcgcgttccaggttcagtgagaaaacttgtctcaaaaatcaga
gggaaaagcaaatgagggtgtcagccatgtgcactcatgcaaatgccatacatgcagaagtatgtgca
cacacacgcacacattaaccaacgactagcaaggaaaatgaaggtggataagaggggtgggactggga
caaaggagggtacctggatgaatatgactgaaggacgttatgtacacatatgaaaacgtcgtactgaa
actcactacaatgtatacttaatatatgctaataaaatatttttaaaagaaaaaaatatccataattg
taaataagaggatcttataattaaaagaccctaaggattc

Capital letters indicate the coding sequence, lower case indicate untranslated bases. ATG start codons that could establish an open reading frame are indicated green. Exon junctions are indicated by an |. Pink letters indicate the central base of the probes of the TaqMan assays used (according manufactures information).

Supplementary Figure 2. Western blot analysis of ABCB1 expression

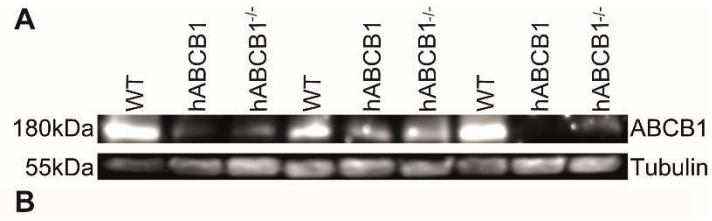

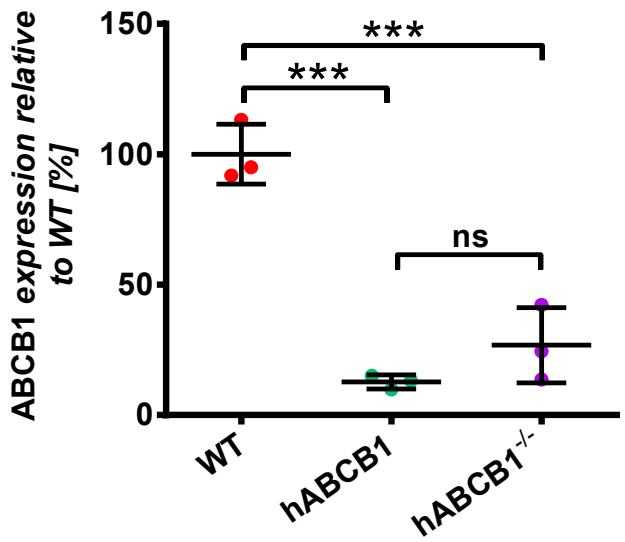

Western blot against ABCB1 confirmed PET imaging findings in hABCB1 animals and shows drastically reduced protein expression of any ABCB1 variant in hABCB1 as well as hABCB1$^{-/-}$ mice. Data are mean ± standard deviation. Statistical significance was determined by 1-way ANOVA with Tukey's Honest Significant Difference post-hoc test, significance level $p<0.05$, *** $p<0.001$.

Supplementary Figure 3. In hABCB1 mice 266 bp of *Abcb1a* are deleted.

```
hABCB1    1 --------------------------------------------------      0
Abcb1a    1 atggaacttgaagaggaccttaagggaagagcagacaagaacttctcaaa     50

hABCB1    1 --------------------------------------------------      0
Abcb1a   51 gatgggcaaaaagaggtagccagattgtttcactttcgtactttacttgt    100

hABCB1    1 --------------------------------------------------      0
Abcb1a  101 cttgtacattcgggcaattagtttgtagcctccagcactgtacttgatta    150

hABCB1    1 --------------------------------------------------      0
Abcb1a  151 gtgggtgttatttcagacttcagaaatgtaaaccagcccttggaaggaac    200

hABCB1    1 --------------------------------------------------      0
Abcb1a  201 tcctcgcttggagcagtccttcaaatgtgtgtgacagatcaatcaatgat    250

hABCB1    1 ----------------ctagagcagcgttgctcacatcttttattttat     34
Abcb1a  251 tctgtgaattcagcctctagagcagcgttgctcacatcttttattttat    300

hABCB1   35 gacctcggctttatgagcgctgttgatcgctcacgcacctgagccatatg     84
Abcb1a  301 gacctcggctttatgagcgctgttgatcgctcacgcacctgagccatatg    350

hABCB1   85 ctgtttgggcgctcactgtggcccattatcttgcttctaataaagccacc    134
Abcb1a  351 ctgtttgggcgctcactgtggcccattatcttgcttctaataaagccacc    400

hABCB1  135 atagatatcacgtttgtggtagaaggaaaagagatccaaataacattttg    184
Abcb1a  401 atagatatcacgtttgtggtagaaggaaaagagatccaaataacattttg    450

hABCB1  185 tttagctctcaatgactatttctatataaaaaggttgtattaccaccgaa    234
Abcb1a  451 tttagctctcaatgactatttctatataaaaaggttgtattaccaccgaa    500

hABCB1  235 agaagccacatcttatattcaaatctctacaaaggctaagtaagtgatta    284
Abcb1a  501 agaagccacatcttatattcaaatctctacaaaggctaagtaagtgatta    550

hABCB1  285 gaactttaatg    295
Abcb1a  551 gaactttaatg    561
```

Alignment of *hABCB1* sequence starting at the first base pair downstream of the loxP insertion site with *Abcb1a* starting at TSS.

Supplementary Figure 4. *Abcb1a* exons 3 and 4 are unaltered.

a)

```
hABCB1-ex3          1 TCCTGGCTCTCATCGGTAACCACATAAGTAGATTTCTAAGATATATTTAC     50
Abcb1a-ex3          1 TCCTGGCTCTCATCGGTAACCACATAAGTAGATTTCTAAGATATATTTAC     50

hABCB1-ex3         51 ATTTAAACTGCATAAATGCCATACCATTATGCTTTTATTGACTAAAACAA    100
Abcb1a-ex3         51 ATTTAAACTGCATAAATGCCATACCATTATGCTTTTATTGACTAAAACAA    100

hABCB1-ex3        101 TAGTCAATTTTGGATTTTGTCTTGTCATTTAACAAAATCTCTGTAAGTTG    150
Abcb1a-ex3        101 TAGTCAATTTTGGATTTTGTCTTGTCATTTAACAAAATCTCTGTAAGTTG    150

hABCB1-ex3        151 ATTTAGTAATTGCAAGGTTTTGTATAAGGTTTTTAAAGTTTCATCTAATT    200
Abcb1a-ex3        151 ATTTAGTAATTGCAAGGTTTTGTATAAGGTTTTTAAAGTTTCATCTAATT    200

hABCB1-ex3        201 ATTCTGCTCTATTTTCAGTAAAAAGGAGAAGAAAGAAAAGAAACCAGCAG    250
Abcb1a-ex3        201 ATTCTGCTCTATTTTCAGTAAAAAGGAGAAGAAAGAAAAGAAACCAGCAG    250

hABCB1-ex3        251 TCAGTGTGCTTACAATGGTGAGTTTTTACTATACTGCCCGCCAATGTCAC    300
Abcb1a-ex3        251 TCAGTGTGCTTACAATGGTGAGTTTTTACTATACTGCCCGCCAATGTCAC    300

hABCB1-ex3        301 TCCTTCTGCTCCTAGAAAAGAGGTAATTCGCCTGGAACAATATGCTA    347
Abcb1a-ex3        301 TCCTTCTGCTCCTAGAAAAGAGGTAATTCGCCTGGAACAATATGCTA    347
```

b)

```
hABCB1-ex4          1 GGGCAGCTTAGACTAGTAGCTAGCAGTCTGGCAAAAATATTTGTGTTTTG     50
Abcb1a-ex4          1 GGGCAGCTTAGACTAGTAGCTAGCAGTCTGGCAAAAATATTTGTGTTTTG     50

hABCB1-ex4         51 GGTGTAGAGGAAAACATCCATGAAACTATCTGATGTCCATGGTTTATTTT    100
Abcb1a-ex4         51 GGTGTAGAGGAAAACATCCATGAAACTATCTGATGTCCATGGTTTATTTT    100

hABCB1-ex4        101 CTTCTCTTTGCAGTTTCGTTATGCAGGTTGGCTGGACAGGTTGTACATGC    150
Abcb1a-ex4        101 CTTCTCTTTGCAGTTTCGTTATGCAGGTTGGCTGGACAGGTTGTACATGC    150

hABCB1-ex4        151 TGGTGGGAACTCTGGCTGCTATTATCCATGGAGTGGCGCTCCCACTTATG    200
Abcb1a-ex4        151 TGGTGGGAACTCTGGCTGCTATTATCCATGGAGTGGCGCTCCCACTTATG    200

hABCB1-ex4        201 ATGCTGATCTTTGGTGACATGACAGATAGCTTTGCAAGTGTAGGAAACGT    250
Abcb1a-ex4        201 ATGCTGATCTTTGGTGACATGACAGATAGCTTTGCAAGTGTAGGAAACGT    250

hABCB1-ex4        251 CTCTAAAAACAGTACTAATATGAGTAAGTATTGTTTGTGGTACAAATTGT    300
Abcb1a-ex4        251 CTCTAAAAACAGTACTAATATGAGTAAGTATTGTTTGTGGTACAAATTGT    300

hABCB1-ex4        301 ACTGGAAATGTGCAAAAAAATCACTCATCTAGAGTAATTATTTGTGGGGC    350
Abcb1a-ex4        301 ACTGGAAATGTGCAAAAAAATCACTCATCTAGAGTAATTATTTGTGGGGC    350

hABCB1-ex4        351 CTTAAAAGGATACACTTCAGTGTTTAGTGGTCTATGTGGTGGGTG    395
Abcb1a-ex4        351 CTTAAAAGGATACACTTCAGTGTTTAGTGGTCTATGTGGTGGGTG    395
```

Alignment of exon 3 (a) and exon 4 (b) as sequenced from hABCB1 mice with *Abcb1a* reference sequence (Gene ID: 18671). Bold letters indicate exons.

Supplementary Table S1: Primers used for amplification and primer walking

Primer	Sequence	Purpose
*ABCB1*_Fw	ACTGGGGACTGTCCTCTTTC	Amplification
*ABCB1*_Rev	CCTCCCCACCATTAAAGTTC	Amplification
forward1	ACT GTC CTC TTT CTG GTT TG	Primer walking
forward2	ACT CAG AGC CGC TTC TTC	Primer walking
forward4	GGA ACT TTG GCT GCC ATC	Primer walking
forward5	GTA GCT GAA GAG GTC TTG	Primer walking
forward6	TGG ACA GGA TAT TAG GAC	Primer walking
forward7	AAG ATC CAG TCT AAT AAG	Primer walking
forward8	TAC TCT TAG CAA TTG TAC	Primer walking
forward9	AGA CGC TGG CTC TGG TG	Primer walking
forward10	TCA ATG GTC AGT GTC CAG	Primer walking
1_reverse1	AGC TGA TAA CTT CGT ATA G	Primer walking
1_reverse2	GTG GGA ATG GTT AAG CAG	Primer walking
forward3.1	AGA AAC CAA CTG TCA GTG	Primer walking
reverse2	TAA TAG GCA TAC CTG GTC	Primer walking
1_reverse3	AGT GGA GAG AAA TCA TAG	Primer walking
*Abcb1a*_Ex02_Fw	TCCTGGCTCTCATCGGTAAC	Amplification
*Abcb1a*_Ex02_Rev	AGCATATTGTTCCAGGCGAA	Amplification
*Abcb1a*_Ex03_Fw	GGGCAGCTTAGACTAGTAGCT	Amplification
*Abcb1a*_Ex03_Rev	CACCCACCACATAGACCACT	Amplification